Research Report

Numerical Fluid Analysis of a Variable Geometry Compressor for Use in a Turbocharger

Yuji Iwakiri, Hiroshi Uchida

ターボチャージャ用可変容量圧縮機の数値流体解析

岩切雄二，内田博

Abstract

A numerical fluid analysis has been used to clarify the cause of the synergistic improvement in the surge limits of a centrifugal compressor when a self-recirculation casing treatment is used together with variable inlet guide vanes.

The following results were obtained by this study.

1) The reverse flow at the tip clearance is closely related to the surge limits, and controlling the reverse flow at the tip clearance is an effective means of improving the surge limits.

2) The surge limit is improved by increasing the recirculation flow rate through the casing treatment.

3) The reverse flow at the tip clearance can be controlled up to the low flow rate region by combining the variable inlet guide vanes with the casing treatment, and as a result, the surge limit is significantly improved.

Keywords Centrifugal compressor, Surge, Casing treatment, Variable inlet guide vane, Computational fluid dynamics (CFD)

要　旨

循環流型ケーシングトリートメントと可変入口案内翼 (VIGV) を組み合わせた場合，遠心圧縮機のサージ限界が相乗的に改善される原因を明らかにする目的で数値流体解析を実施し，以下の結果を得た。

1) チップクリアランス部の逆流とサージ限界とは強い相関があり，この逆流を抑制することがサージ限界の改善に効果的である。

2) ケーシングトリートメントによる循環流量が増加するとサージ限界が改善する傾向がある。

3) ケーシングトリートメントとVIGVを組み合わせることでクリアランス部の逆流がより少流量域まで抑制され，その結果サージ限界が大幅に改善する。

キーワード　遠心圧縮機，サージ，ケーシングトリートメント，可変入口案内翼，数値流体解析

特集

1. Introduction

Lately, in order to improve engine performance, manufacturers have been developing high-pressure turbocharging technology. To realize high-pressure turbocharging from the low flow rate, it is necessary to improve the surge limits of the compressor. Therefore, many researches[1-4] have been done to improve the surge limits.

We discovered, through experiment, that the surge limit could be greatly improved by combining a self-recirculation type casing treatment with variable inlet guide vanes (VIGV), relative to using each independently. In this study, the influence both of the casing treatment and the VIGV on the flow in a centrifugal compressor was examined by means of three-dimensional numerical fluid analysis.

The numerical analysis showed that the reverse flow near the tip clearance around the impeller inlet, which cannot be controlled by the casing treatment alone, is suppressed by using the VIGV together with the casing treatment.

2. Structure of the compressor

Figure 1 shows a meridional section of the compressor used for this study. The applied casing treatment is of the self-recirculation type that is commonly used for turbochargers. It has a suction slit near the inducer throat of the impeller and a discharge slit upstream of the impeller inlet. A feature of this casing treatment is the curve in the wall surface of the cavity which converts kinetic energy into pressure energy with only a small pressure loss. In addition, radial ribs are arranged to suppress the tangential velocity component at the outlet of the casing treatment. The VIGV is an axial flow type with 7 vanes. The vane setting angle of the VIGV can be adjusted between 0 and 80 degrees from the axial direction.

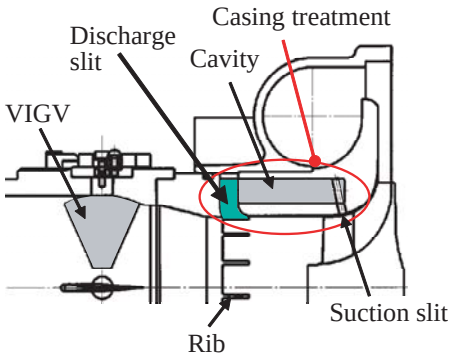

Fig. 1 Cross section of the compressor.

3. Numerical calculation method and conditions

We carried out a three-dimensional numerical fluid analysis for the steady state condition that considered viscosity, compressibility and turbulence. We investigated the flow field in the compressor by using the commercial STAR-CD CFD code. The standard k-ε turbulence model was used with wall functions. An example of the computational grid is shown in **Fig. 2**. The compressor scroll was not included in the analysis domain, but a full pitch model was applied because the number of cavities differed from the number of impeller blades. We used a total of around one million calculation grid points for the compressor with both the VIGV and the casing treatment. The impeller tip clearance was divided into 7 layers to consider the flow in the tip clearance. Since we applied the multi-frame implicit solution method, the boundary values on the connected surfaces of the stationary and rotational parts were not input. The air flow rate and impeller rotation speed were given. The restraint condition of there being no backward flow at the exit boundary was given. Using this condition enables us to perform the calculation for a flow rate less than the surge flow rate.

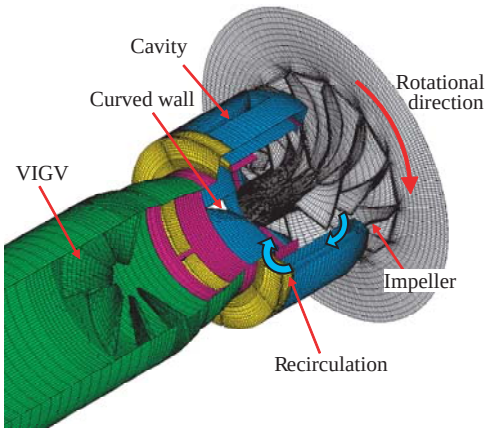

Fig. 2 Computational grid (surface).

4. Results and discussion

4. 1 Effects of the casing treatment

First, the calculation accuracy was investigated by comparing the calculated values with those obtained by experiment. It can judge whether the energy input by the impeller can be calculated accurately by comparing the temperature ratio of the compressor exit and the inlet. The temperature ratio at a rotational speed of $N=0.88N_{ref}$ is shown in **Fig. 3**. Here, N_{ref} is the design speed. WOCT means "without the casing treatment," while CT means "with the casing treatment." CT2 has a suction slit that is 20 % wider than that of CT1. The temperature ratio of CT2 is higher than that of WOCT in the low flow rate region. This resulted from the rise of the impeller inlet air temperature caused by the recirculation flow of the casing treatment. The difference between the experiments and the calculations is 1 % or less for all the calculation points. This means that the flow in the compressor, including the influence of recirculation, can be calculated with high accuracy using this CFD.

The experiment and calculation results for the compressor characteristics are shown in **Fig. 4**. Since the scroll is not included in the calculation domain, the pressure loss of the scroll is not considered in the calculation. Therefore, the pressure ratios of the calculation results are higher than those of the results obtained by experiment. They do, however, correspond to the results of the experiments qualitatively. The pressure ratio of CT2 is higher than that of WOCT in the low flow rate region.

Next, the improvement of the flow in the impeller as caused by the casing treatment is described. The meridional velocity vectors and relative Mach number distributions in the impeller at a flow rate of $G=0.64G_{ref}$ are shown in **Fig. 5**. Here, G_{ref} is the design flow rate. This condition is equivalent to the surge limit of WOCT. The indicated surface is the center of the full blade's suction surfaces and the splitter blade's pressure surface. There is a low-speed region at the shroud side in the case of

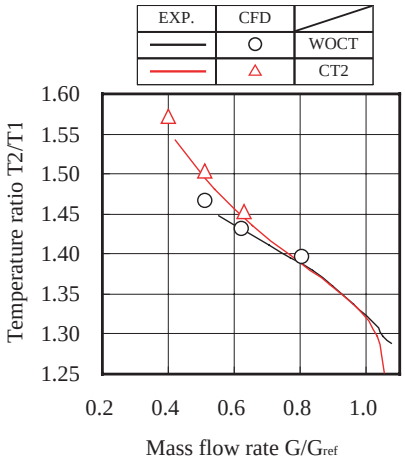

Fig. 3 Comparison of temperature ratio of experiments and calculations ($0.88N_{ref}$).

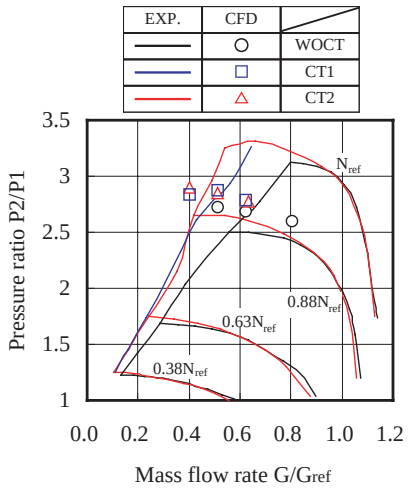

Fig. 4 Comparison of pressure ratio of experiments and calculations.

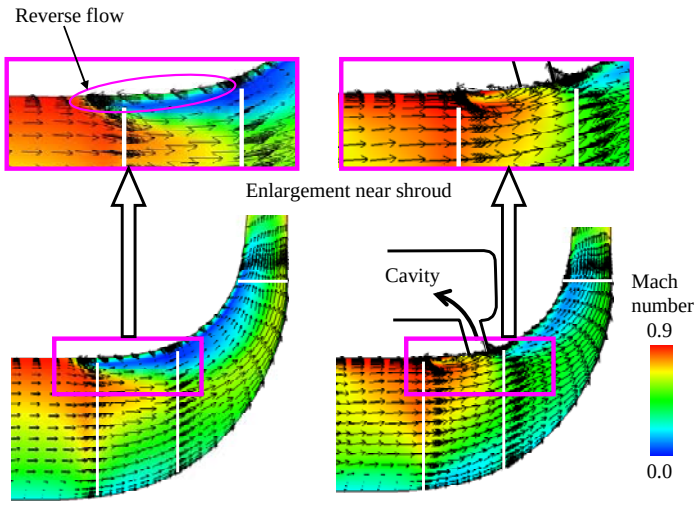

a) Without the casing treatment b) With the casing treatment (CT1)

Fig. 5 Effect of the casing treatment on reverse flow control ($0.64G_{ref}$, $0.88N_{ref}$).

特集

WOCT, and the reverse flow at the tip clearance reaches a point upstream of the full blade's leading edge. In the case of CT1, the low speed region is limited to around the splitter blade. The air near the tip clearance is sucked into the suction slit, and the reverse flow at a point upstream of the full blade's leading edge is controlled. In the flow path between the suction slit and the discharge slit of the casing treatment, the passing air flow rate is increased as a result of the recirculation flow of the casing treatment. Because of this, the attack angle is reduced, and the flow inside the impeller is improved. This leads to a rise in the pressure ratio.

The influence of the width of the suction slit on the flow in the impeller is shown in **Fig. 6**. The air flow rate is $G=0.51G_{ref}$, which is the surge limit of CT1. Under this condition, the reverse flow of the CT1 through the tip clearance reached a point upstream of the leading edge. On the other hand, the reverse flow is suppressed in the case of CT2, which has a wider suction slit.

The relationship between the air flow rate and the recirculation flow rate of the casing treatment calculated by CFD is shown in **Fig. 7**. The vertical axis indicates the ratio of the recirculation flow rate for the air flow rate. As shown in the figure, the ratio of the recirculation flow increases with a reduction in the air flow rate. The recirculation flow rate of CT1 is smaller than that of CT2 at an air flow rate of $G=0.4G_{ref}$. From the results of the experiments on the surge limits, we found that the surge limits of CT1 deteriorate at a pressure ratio of 2.5 or higher, relative to CT2. It is thought that an increase in the recirculation flow rate will be effective in improving the surge limits.

The recirculation flow rate of CT1 was less than that of CT2 only when $G=0.4G_{ref}$. Here, we consider the reason for this. **Figure 8** shows the static pressure on the shroud near the suction slit. Zero of the horizontal axis corresponds to the leading edge of the main blade. The static pressure distribution of CT1 and CT2 is similar at an air flow

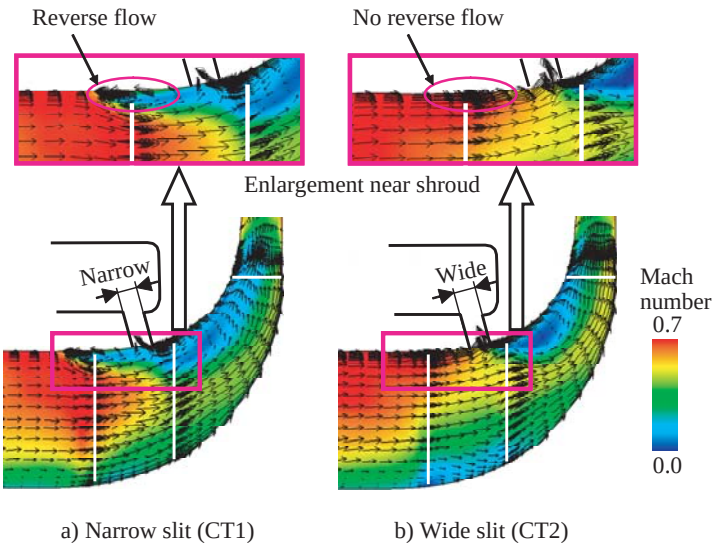

Fig. 6 Effect of width of the suction slit on reverse flow ($0.51G_{ref}$, $0.88N_{ref}$).

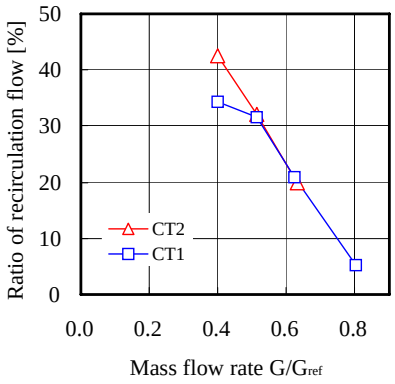

Fig. 7 Recirculation flow rate through the cavity ($0.88N_{ref}$, CFD).

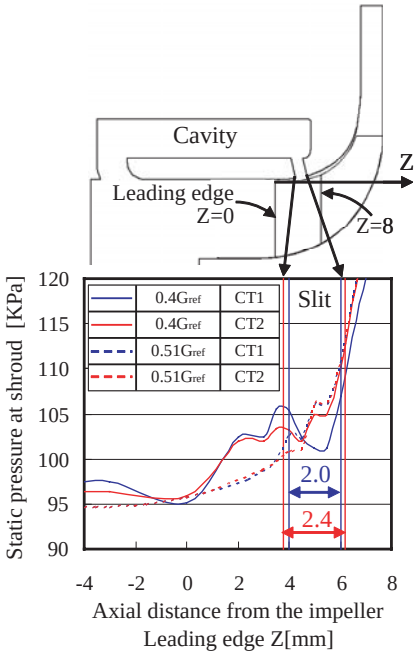

Fig. 8 Static pressure distributions at shroud ($0.88N_{ref}$, CFD).

rate of G=0.51G_{ref}. On the other hand, the static pressure of CT1 is lower than that of CT2 at the suction slit at an air flow rate of G=0.4G_{ref}. We assume that the drop in the static pressure at the suction slit of CT1 causes the reduction of the recirculation flow rate compared with CT2 at an air flow rate of G=0.4G_{ref}, as shown in Fig. 7.

Figure 9 shows the velocity vectors and Mach number distributions near the suction slit. The reverse flow near the shroud is left upstream of the suction slit of CT1.

Next, the influence of the arrangement of the discharge ribs was considered. The velocity vectors in the cavity of the casing treatment at an air flow rate of G=0.4G_{ref} are shown in **Fig. 10**. The indicated surface is a cylindrical section near the outermost diameter of the cavity. The air that is sucked into the suction slit flows to the discharge slit in accordance with the curved cavity wall. On the other hand, the reverse flow occurs near the wall of the other side that is not curved. The ribs are arranged in order to diminish the tangential velocity component of the recirculation flow at the discharge slit of the casing treatment. There are inflows and outflows at adjacent cavities of CT2 since the boundary of the cavity and the position of the rib are different from each other. And, it is thought that this causes the reverse flow in the cavity to increase.

Given that we expected an increase in the recirculation flow, we arranged the phase of the boundary of the cavity and the rib. The results of the calculations are shown in Fig. 10b. The reverse flow domain becomes small, and ratio of the recirculation flow rate for the compressor air flow rate has increased up to approximately 48 %. Accordingly, the surge limit was improved by about 15 % at pressure ratios in excess of 2.5.

4. 2 Effects of combination with the VIGV

The compressor characteristics when the VIGV is combined with CT2 are shown in **Fig. 11**. A numerical analysis was performed using each of the casing treatment and VIGV separately, and then both together. "V70" in the figure indicates a "VIGV setting angle of 70 degrees," while

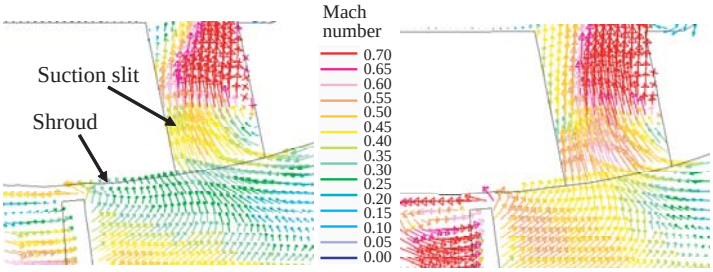

a) Narrow slit (CT1) b) Wide slit (CT2)

Fig. 9 Velocity vector distributions near the suction slit (0.4G_{ref}, 0.88N_{ref}).

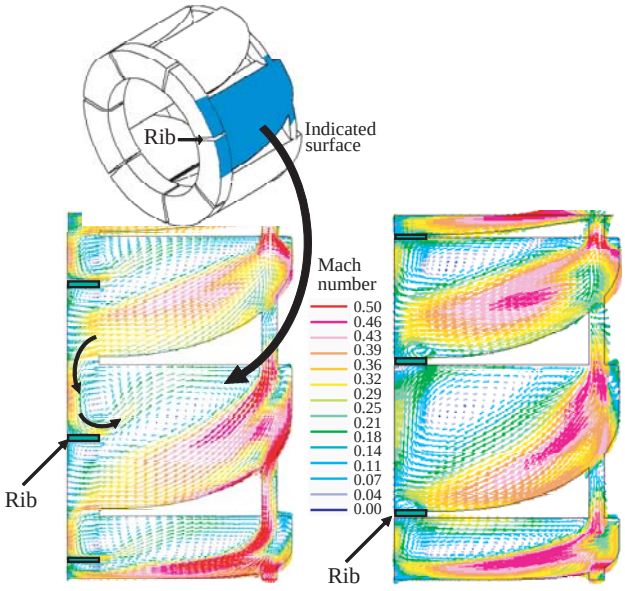

a) Different rib phase (CT2) b) Same rib phase (CT2R)

Fig. 10 Velocity vector distributions in the cavity (0.4G_{ref}, 0.88N_{ref}).

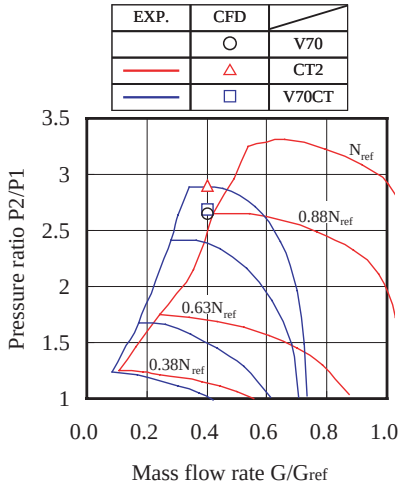

Fig. 11 Comparison of pressure ratio of experiments and calculations with the VIGV.

"V70CT" is a "combination with the VIGV setting angle of 70 degrees and CT2."

The velocity vectors and relative mach number distributions in the impeller at an air flow rate of $G=0.4G_{ref}$ are shown in **Fig. 12**. This calculation condition is equivalent to the surge limit of CT2. The reverse flow at the tip clearance cannot be controlled completely with CT2 alone, and part of the reverse flow reaches a point upstream of the impeller inlet. Although the low-speed region downstream of the splitter blade is reduced by the VIGV, the reverse flow near the shroud is not controlled, and it reaches a point upstream of the impeller inlet. On the other hand, when it is combined with the VIGV at a setting angle of 70 degrees, the low-speed region on the shroud side is also reduced downstream of the suction slit, while the flow between the shroud and hub is equalized, comparatively.

The relationship between the total pressure loss of the VIGV and air flow rate is shown in **Fig. 13**. The pressure loss at a VIGV setting angle of 0 degrees can be neglected up to a high flow rate. For a VIGV setting angle of 80 degrees, the pressure loss increases rapidly with an increase in the air flow rate. Although the pressure loss at an air flow rate of $G=0.29G_{ref}$ is equivalent to a drop of about 5 points in the compressor efficiency, the impeller efficiency improves thanks to the improvement in the flow caused by the pre-whirl of the VIGV. As a result, the efficiency of the compressor with the VIGV is similar to that without the VIGV at low flow rates.

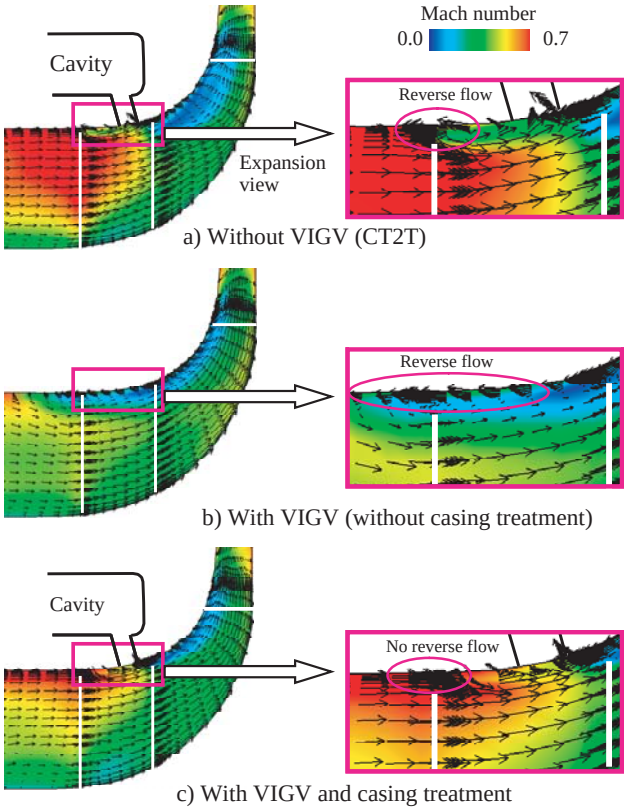

Fig. 12 Effect of combination of the casing treatment and the VIGV on reverse flow ($0.4G_{ref}$, $0.88N_{ref}$).

5. Conclusion

The influence of the casing treatment and the variable inlet guide vanes on the surge limits of the centrifugal compressor was clarified through both experiment and CFD.

(1) The reverse flow at the tip clearance is closely related to the surge limits, and controlling the reverse flow at the tip clearance is effective means of improving the surge limit.

(2) There is a tendency for the surge flow rate to decrease with an increase in the recirculation flow rate through the casing treatment. Moreover, the recirculation flow rate is increased by expanding the width of the suction slit and arranging the phase of the rib and the boundary of the cavity. As a result, the surge limit is improved.

(3) The recirculation flow through the casing treatment incurs a small pressure loss due to the curvature of the cavity wall. Because of this, the compressor efficiency in the low flow rate region is improved through the use of the casing treatment.

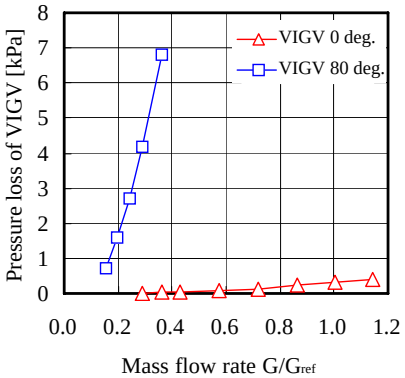

Fig. 13 Pressure loss of the VIGV ($0.63N_{ref}$, CFD).

(4) The reverse flow at the tip clearance can be controlled up to the low flow rate region by combining the VIGV with the casing treatment and, as a result, the surge limit is significantly improved.

References

1) McKee, R. J. and Deffenbaugh, D. M. : "Factors That Affect Surge Precursors in Centrifugal Compressors", GMRC Gas Machinery Conf., Salt Lake City, UT, (2003)
2) Yamaguchi, S., et al. : "The Development of Casing Treatment for Turbocharger Compressor", 7th Int. Conf. on Turbochargers and Turbocharging, Proc. of IMechE C602/016/2002, (2002)
3) Tange, H., Ikeya, N. and Takahashi, M. :"Varibable Geometry of Turbocharger Compressor for Passenger Vehicles", SAE Tech. Pap. Ser., No.2003-01-005 (2003)
4) Whitfield, A. and Abdullah, A. H. : "The Performance of a Centrifugal Compressor with High Inlet Prewhirl", ASME Pap. No.97-GT-182 (1997)

(Report received on Jun. 21, 2006)

Yuji Iwakiri
Research fields : Turbomachine, Aerodynamics
Academic society : Jpn. Soc. Mech. Eng.

Hiroshi Uchida
Research fields : Turbomachine, Aerodynamics
Academic society : Gas Turbine Soc. Jpn.
Awards : The Outstanding Technical Paper Awards of Gas Turbine Soc. Jpn., 2002